Stratospheric ozone changes from explosive tropical volcanoes: Modelling and ice core constraints

Alison Ming[1,2], V. Holly L. Winton[1], James Keeble[2,3], Nathan L. Abraham[2,3], Mohit C. Dalvi[4], Paul Griffiths[2,3], Nicolas Caillon[5], Anna E. Jones[1], Robert Mulvaney[1], Joël Savarino[5], Markus M. Frey[1], Xin Yang[1]

[1]British Antarctic Survey, Cambridge, CB3 0ET, UK
[2]Department of Chemistry, University of Cambridge, Cambridge, UK
[3]National Centre for Atmospheric Science (NCAS), University of Cambridge, Cambridge, UK
[4]Met Office Hadley Centre, Exeter, UK, EX1 3XB
[5]Université Grenoble Alpes, CNRS, IRD, Grenoble INP, IGE, F-38000 Grenoble, France

Key Points:

- The tropical volcanic eruption in the model shows that the sign of the ozone change is highly sensitive to stratospheric chlorine amounts.
- $\delta^{15}N(NO_3^-)$ (a proxy for surface ultra-violet radiation) from the Samalas 1257 eruption is obscured by inter-annual variability in the ice core.
- Any $\delta^{15}N(NO_3^-)$ signal from the Samalas eruption will be below 60 per mil. It is unlikely that prolonged complete ozone removal occurred.

Corresponding author: Alison Ming, `A.Ming@damtp.cam.ac.uk`

Abstract

Major tropical volcanic eruptions have emitted large quantities of stratospheric sulphate and are potential sources of stratospheric chlorine although this is less well constrained by observations. This study combines model and ice core analysis to investigate past changes in total column ozone. Historic eruptions are good analogues for future eruptions as stratospheric chlorine levels have been decreasing since the year 2000. We perturb the pre-industrial atmosphere of a chemistry-climate model with high and low emissions of sulphate and chlorine. The sign of the resulting Antarctic ozone change is highly sensitive to the background stratospheric chlorine loading. In the first year, the response is dynamical, with ozone increases over Antarctica. In the high HCl (2 Tg emission) experiment, the injected chlorine is slowly transported to the polar regions with subsequent chemical ozone depletion. These model results are then compared to measurements of the stable nitrogen isotopic ratio, $\delta^{15}N(NO_3^-)$, from a low snow accumulation Antarctic ice core from Dronning Maud Land (recovered in 2016-17). We expect ozone depletion to lead to increased surface ultraviolet (UV) radiation, enhanced air-snow nitrate photo-chemistry and enrichment in $\delta^{15}N(NO_3^-)$ in the ice core. We focus on the possible ozone depletion event that followed the largest volcanic eruption in the past 1000 years, Samalas in 1257. The characteristic sulphate signal from this volcano is present in the ice-core but the variability in $\delta^{15}N(NO_3^-)$ dominates any signal arising from changes in UV from ozone depletion. Prolonged complete ozone removal following this eruption is unlikely to have occurred over Antarctica.

Plain Language Summary

Chlorine in the stratosphere destroys ozone that protects the Earth from harmful ultraviolet radiation. Volcanic eruptions in the tropics can emit sulphate and chlorine into the stratosphere. Chlorine levels are currently decreasing and to understand the impact of a volcanic eruption on stratospheric ozone in a future climate, historical eruptions are a useful analogue since the pre-industrial climate also had low chlorine levels. Using a chemistry climate model, we run a set of experiments where we inject different amounts of sulphate and chlorine into the stratosphere over the tropics to simulate different types and strengths of explosive volcanoes and we find that the ozone over Antarctica initially increases over the first year following the eruption. If the volcano emits a large amount of chlorine, ozone then decreases over Antarctica in years two to four following the eruption. We also compare our results to ice-core data around a large historic volcanic eruption, Samalas (1257).

1 Introduction

The ozone layer protects life on Earth from ultraviolet (UV) radiation. Explosive tropical volcanic eruptions can inject volcanic gases into the stratosphere which can disrupt the complex stratospheric chemistry and lead to substantial changes in total column ozone (Solomon, 1999; Robock & Oppenheimer, 2003, for a comprehensive review). Over the last 1000 years, a number of explosive tropical volcanoes have injected copious volumes of sulphur dioxide (SO_2) and hydrochloric acid (HCl) into the stratosphere. Injection of sulphur dioxide into the stratosphere from an explosive volcanic eruption increases the number of sulphate aerosol particles, providing a larger surface area for heterogeneous reaction to take place on. The impact of this change in stratospheric aerosol loading on ozone is dependent on the stratospheric chlorine loading (e.g., Timmreck, 2012). In a low chlorine atmosphere, N_2O_5 reacts with water vapour on the surfaces of these volcanic aerosols to form HNO_3, effectively sequestering reactive NO_x species into a long-lived reservoir and limiting the availability of NO_x radicals to take part in catalytic reactions which deplete stratospheric ozone

(Crutzen, 1970; Johnston, 1971). However, in a high chlorine atmosphere, while the heterogeneous reaction of N_2O_5 on aerosol surfaces has the same effect, halogenated reservoir species also undergo heterogeneous reactions, liberating reactive ClO_x and BrO_x species from long-lived reservoirs (e.g., Solomon, 1999). As a result, a large sulphur dioxide injection is expected to cause polar ozone loss when the chlorine loading of the stratosphere is high (e.g. Tie & Brasseur, 1995), while in a low chlorine environment, such as a pre-industrial atmosphere or a future atmosphere where the chlorine loading of the stratosphere has declined, it is widely accepted that an injection of sulphate from an explosive tropical volcanic eruption will lead to ozone gain over polar regions (Langematz et al., 2018, and references therein). To understand the future atmospheric impact of volcanic eruptions, studying historic eruptions is a useful analog.

Estimates of the amount of sulphur dioxide emitted into the stratosphere from eruptions over the past 1000 years are highly variable. For example, sulfate mass concentration records from ice core data give the following estimates for recent tropical eruptions: ~ 10 to $20\,Tg\ SO_2$ from Mount Pinatubo in 1991 (Timmreck et al., 2018), $\sim 60\,Tg\ SO_2$ from Mount Tambora in 1815 (Zanchettin et al., 2016) and ~ 100 to $140\,Tg\ SO_2$ from the Samalas 1257 series of eruptions (1257, 8.4° S, 116.5°E) (Toohey & Sigl, 2017). Samalas is the largest eruption over the last 1000 years and part of a series of 4 large eruptions occurring over a period of about 26 years.

Some types of explosive volcanoes also emit chlorine and other halogen compounds. Volcanic stratospheric chlorine emissions are important for ozone destruction reactions (Kutterolf et al., 2013) but are less well constrained, since the highly soluble HCl is scavenged by processes in the volcanic plume (Halmer et al., 2002). In the stratosphere, HCl is the dominant chlorine reservoir species and a source of reactive halogen such as chlorine monoxide, ClO, that destroys ozone. A sophisticated plume model (Textor et al., 2003) suggest that 10% to 20% of the HCl emitted would enter the stratosphere and recent satellite observations have detected HCl injection into the stratosphere from explosive volcanoes (Theys et al., 2014). Geo-chemical evidence by Vidal et al. (2016) suggests that the Samalas eruption could have injected as much as $\sim 230\,Tg$ HCl into the atmosphere. In contrast, observations during the 1991 Pinatubo eruption show that the efficiency of the scavenging is highly dependent on atmospheric conditions with barely detectable increases in stratospheric HCl following the eruption (Wallace & Livingston, 1992). Volcanic HCl emissions and the fraction of HCl mass entering the stratosphere are hence highly variable as these depend on the geochemistry of the eruption and the efficiency of the scavenging processes respectively. The type and location of the eruption also play a role.

The impact of an explosive eruption on stratospheric ozone also depends on dynamical processes. Variability arising from the El Niño-Southern Oscillation (ENSO), the quasi-biennial oscillation (QBO) and the variability in the Brewer-Dobson circulation are able to affect the ozone response following the eruption (Lehner et al., 2016; Telford et al., 2009). In addition, the radiative heating from the aerosol injection and associated changes to the planetary wave flux from the troposphere are able to alter the stratospheric circulation and hence the transport of aerosols and trace gases (Poberaj et al., 2011). Since the precise time of the year of the historic eruption is often not known, these factors have to be taken into account in the model simulations (Stevenson et al., 2017).

Ground-based observations of total column ozone (TCO) commenced in the 1920s and captured the severe decline in the ozone layer resulting from anthropogenic production of long-lived ozone destroying-halocarbons (e.g., Harris et al., 2015, and references therein). However, beyond the relatively short instrumental period, records of total column ozone are non-existent and thus paleo-reconstructions are required to under-

stand how natural phenomena, such as volcanic eruptions, can impact the variability of total column ozone.

Recent research has focused on novel Antarctic ice core proxies of surface UV radiation, which can provide constraints on past ozone variability as changes in total column ozone affect the surface UV over Antarctica. The UV proxy is based on the stable isotopic composition of nitrate ($\delta^{15}N(NO_3^-)$) at low accumulation sites in Antarctica (Frey et al., 2009). Theory, laboratory and field experiments have shown that nitrate (NO_3^-) loss from snow and associated isotopic enrichment of $\delta^{15}N(NO_3^-)$ in the NO_3^- fraction remaining in the snow is driven by UV photolysis (Shi et al., 2019; Berhanu et al., 2014, 2015; Frey et al., 2009). The presence of the heavier isotope of nitrogen, ^{15}N, in NO_3^- leads to an increase in reduced mass which causes a red shift in the vibrational frequencies and a reduction in zero point energy. The UV absorption peak of the heavier isotope is then narrower and blue shifted resulting in a difference in isotopic fractionation. Further details of this process can be found in Frey et al. (2009). The photolytically-induced fractionation of the $\delta^{15}N(NO_3^-)$ signal is eventually archived in firn and ice. This depends on a number of site-specific factors aside from the UV irradiance including the snow physical properties and the amount and timing of snow accumulation (Erbland et al., 2015, 2013; Noro et al., 2018; Shi et al., 2018). The largest enrichment of $\delta^{15}N(NO_3^-)$ is observed at low accumulation sites on the East Antarctic Plateau, where near surface snow is exposed for more than one summer season to incoming UV radiation (Erbland et al., 2013; Shi et al., 2018).

Winton et al. (2019) carried out a comprehensive field and modelling study of the air-snow transfer of NO_3^- at the low snowfall accumulation site at Kohnnen Station in Dronning Maud Land (DML), East Antarctica as part of the ISOL-ICE (ISotopic constraints of past Ozone Layer in polar ICE) project. At the DML site, NO_3^- is recycled three times before it is archived in the snowpack below a depth of 15 cm and within 0.75 years. Sensitivity analysis with a 1D air-snow model, TRANSITS (TRansfer of Atmospheric Nitrate Stable Isotopes To the Snow) (Erbland et al., 2015), of $\delta^{15}N(NO_3^-)$ at DML showed that the dominant factors controlling the archived $\delta^{15}N(NO_3^-)$ signature are the snow accumulation rate and e-folding depth of the surface snowpack for incident UV, with a smaller role from changes in the snowfall timing and TCO. The Winton et al. (2019) study sets the framework for the interpretation of a $\delta^{15}N(NO_3^-)$ record from the new ISOL-ICE ice core drilled in January 2017 at Kohnen Station in Dronning Maud Land, henceforth referred to as the DML site, following the terminology in Winton et al. (2019). The DML region experiences low annual accumulation rates ($< 10 \, \mathrm{g \, cm^{-2} \, yr^{-1}}$) but ice cores from the area still record seasonal, centennial and millennial scale variability in glaciochemistry (Göktas et al., 2002; Oerter et al., 2000; Sommer et al., 2000), as well as highly-resolved tropical volcanic eruptions (Hofstede et al., 2004; Severi et al., 2007). This site offers useful potential to investigate the impact of volcanic eruptions on TCO, surface UV radiation and its imprint in the $\delta^{15}N(NO_3^-)$ ice core signature.

The aim of this study is to combine modelling studies with ice core evidence to understand the impact on the total column ozone of explosive tropical volcanic eruptions in a low chlorine stratosphere. The first part of this study will explore the sensitivity of ozone over Antarctica to different volcanic emission scenarios using a state-of-the-art chemistry-climate model (UM-UKCA) with additional key heterogeneous and photolysis reactions. The second part of the study examines the $\delta^{15}N(NO_3^-)$ signal for the tropical volcanic eruption, Samalas. Section 2 described the methods used in this paper. We provide a brief overview of the UM-UKCA chemistry-climate model and the additional key heterogeneous and photolysis reactions that were added to improved the representation of stratospheric ozone. A Pinatubo eruption test case is used to validate the response to a present day volcanic eruption. We also provide a brief description of the ice core data and the isotopic analysis. In Section 3.1, we

use the model to investigate the response of stratospheric ozone to various volcanic emission scenarios in a pre-industrial atmosphere. The isotopic constraints offered on past ozone change from the ice core evidence are presented in Section 3.2. Finally, Section 4 combines the model results and ice core analysis to discuss the implications for past and future ozone changes from explosive tropical volcanoes.

2 Data and methods

2.1 Model description, changes

We make use of the coupled chemistry-climate model which consists of the United Kingdom Chemistry and Aerosol (UKCA) module together with the UK Met Office Unified Model (UM) (Walters et al., 2019; Morgenstern et al., 2009; O'Connor et al., 2014). The model is free running and with prescribed sea ice and sea surface temperatures. The original configuration is similar to the Atmospheric Model Intercomparison Project (AMIP) simulation of UK Earth system model (UKESM) submission to the Coupled Model Intercomparison Project Phase 6 (CMIP6) (Eyring et al., 2016). The resolution is 1.875° longitude by 1.25° latitude with 85 vertical levels extending from the surface to 85 km. The UKCA module is run with the combined stratosphere and troposphere chemistry (CheST) option at version 10.9. The model has an internally generated QBO and the dynamics of the stratosphere are well represented (Osprey et al., 2013). The model includes the aerosol scheme, GLOMAP-mode, to simulate the direct and indirect radiative effects (Mann et al., 2010). Aerosol optical properties are computed online as the particle size distributions evolve due to micro-physical processes.

Stratospheric ozone concentrations are determined by sets of photo-chemical reactions first described by Chapman (1930) plus ozone destroying catalytic cycles involving chlorine, nitrogen, hydrogen and bromine radical species (Solomon, 1999). The photolysis reactions in the model make use of rates calculated from a combination of the FAST-JX scheme (Wild et al., 2000; Bian & Prather, 2002; Neu et al., 2007) and look-up tables. FAST-JX wavelengths range from 177 to 850 nm over 18 bins and calculates scattering for all bands (Telford et al., 2013). Above about 60 km, a look-up table of photolysis rates (Lary & Pyle, 1991; Morgenstern et al., 2009) is used when wavelengths below 177 nm become important. Heterogeneous reactions are also important for determining stratospheric ozone concentrations in the presence of polar stratospheric clouds in the polar lower stratosphere or in the presence of sulphate aerosol following explosive volcanic eruptions. Ozone depleting radicals are produced by the photolysis of the products formed from halogen containing compounds reacting on the surface of stratospheric aerosol such as polar stratospheric clouds. These species include hydrochloric acid (HCl), chlorine nitrate ($ClONO_2$), hydrogen bromide (HBr) and bromine nitrate ($BrONO_2$). Three types of aerosol are considered by the model: ice, nitric acid trihydrate and sulfate aerosol. Above a temperature of about 195 K, reactions occur on liquid sulfate aerosol, around 195 K to 188 K, the model forms nitric acid trihydrate particles and below about 188 K, ice particles form.

We add 8 new heterogeneous reactions to the model involving chlorine and bromine species in a similar way to Dennison et al. (2019), following the previous work by (Yang et al., 2014), with the main difference being the explicit treatment of the reactions of 4 additional chemical species: Cl_2, Br_2, $ClNO_2$ and $BrNO_2$. These species are also photolysed to produce Cl and Br radicals. Reaction rates depend on the probability of a gas molecule colliding irreversibly with the surface of the aerosol and this is given by an uptake coefficient. We update the calculation of the uptake coefficients using the same scheme as Dennison et al. (2019) with the differences listed in Table A1 in the Appendix. The model data used in this paper is archived on the Centre for Environmental Data Analysis (Ming, 2020).

2.2 Model validation

The changes to the stratospheric chemistry are tested by running the model for 30 years in a year 2000 time slice experiment using CMIP6 prescribed trace gases and sea surface temperature forcings. The model is mostly able to reproduce the observed total column ozone and the results are similar to those found by Dennison et al. (2019) in which a more thorough discussion of the changes can be found. The improved match with observed TCO resulting from our model updates is shown in Figure 1(a). The spring ozone hole over Antarctica is deeper than the original model with total column ozone values reaching about 175 DU (65 to 90° S average) in October compared to about 200 DU in the original model. These values are closer to those in the ozone values from the satellite ozone dataset from the National Institute of Water and Atmospheric Research – Bodeker Scientific (NIWA-BS) satellite dataset (version 3.4; see `http://www.bodekerscientific.com/data/total-column-ozone`). The ozone hole minimum in the satellite data reaches about 185 DU although this happens earlier in September. The modified model still under predicts the summer ozone values which take longer to recover compared to observations. This could be due to the vortex breakup being delayed and is a known issue in a number of comprehensive chemistry climate model (Eyring et al., 2010; Butchart et al., 2011; McLandress et al., 2012). Overall, our changes to the chemistry scheme lead to an ozone distribution that is very similar to Dennison et al. (2019).

To assess the model response to a volcanic perturbation in the present atmosphere we run an experiment that simulates the eruption of Mount Pinatubo. The model is first spun up using CMIP6 present day forcings, including changing trends in trace gases. We then initialize four ensemble runs using the climate state taken from four different years of the spun up model state. The runs use the CMIP6 trace gas forcings from 1979 to 1994 with the eruption happening in 1991. Although the exact climate state at the time of the Pinatubo eruption is known from observations, the four ensemble runs are done so as to span over the variability arising from the QBO and ENSO. This allows the Pinatubo run to be compared to the pre-industrial volcanic runs in Section 3.1. The timing of historical volcanic eruptions is not well constrained and we do not know the phases of the QBO and ENSO in which the eruptions occurred. The ensemble is designed to average over this variability. We simulate the Pinatubo eruption as an emission of 10 Tg SO_2 and 0.02 Tg HCl on 1 June 1991 into the stratosphere as a single vertical plume between 19 and 24 km altitude (the neutral buoyancy height of the plume) at 15.1 °N and 120.2 °E. Mills et al. (2016) discuss the justification for various choices of modelling parameters for Pinatubo. The aim of this experiment is not to reproduce the observations after the Pinatubo eruption exactly but to check that, with the additional chemical reactions and emissions, our model is still able to simulate the broad pattern of the ozone response after a current day explosive volcano.

Figure 1(b) shows change in total column ozone from the Pinatubo eruption in the NIWA-Bodeker dataset as the difference between a 1991 to 1994 average and a climatology taken from 1979 to 1990. Similarly, the same change in the model runs is shown in Figure 1(c) but using the average of the four ensemble runs from 1991 to 1994 and a climatology taken from 1979 to 1990. A non parametric permutation test is used to determine if the changes seen are larger than the natural variability; changes below the level of the noise is represented by the grey fog which is plotted as overlaid contours at confidence levels of 95, 90, 80, 70 and 60%. The same test is used in all subsequent model plots. The red triangle marks the volcanic eruption in this and subsequent plots.

The initial, low latitude, increase in total column ozone south of the volcano in the year following the eruption and the decrease in ozone in Jan 1992 over the North Pole are captured by the model although the changes are shorter lived than in

the satellite data. Note that the Antarctic ozone hole is not as prominent a feature in model runs due to the averaging of four ensemble members. Our model ozone changes are qualitatively similar to the Pinatubo case study by Aquila et al. (2012) using a different chemistry-climate model. Aquila et al. (2012) also discuss, in more detail, the possible mechanisms for the stratospheric ozone changes. This experiment demonstrates that our modified model is able to satisfactorily stimulate the ozone changes associated with a present-day volcanic eruption.
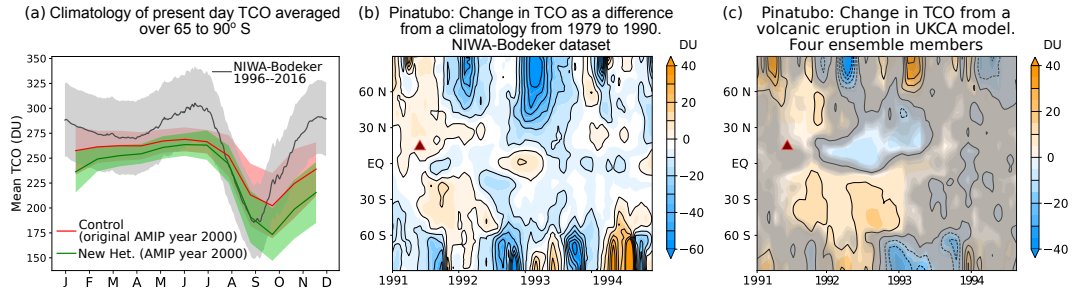
Figure 1. (a) Climatology of total column ozone (TCO) (DU) for the present climate from the NIWA-Bodeker satellite dataset (1996–2016) in black, a 30 year timeslice run of the year 2000 from the original AMIP model setup in red and the corresponding timeslice with the modified model with new heterogeneous reactions and emission files in green. Shaded bands show ±1 standard deviation. (b) Change in Bodeker ozone following the Pinatubo eruption (red triangle) as a difference from a climatology taken from years 1979 to 1990. The QBO signal has been filtered out. (c) Change in TCO (DU) following the Pinatubo eruption (10 Tg SO_2, 0.02 Tg HCl) in the model. The plot shows the difference from a climatology taken from 1979 to 1990 and is the average of four ensemble members. The grey fog illustrates regions where the signal is below the level of the noise (see the main text for further details). The red triangle marks the volcanic eruption. Note the different colour scales between (b) and (c).

2.3 Ice core analysis

The first high-resolution record of $\delta^{15}N(NO_3^-)$ was obtained for the last 1.3 kyr from the 120 m ISOL-ICE ice core. The core was drilled in the clean air sector at Kohnen Station, DML on the high-elevation East Antarctic Plateau (2892 m above sea-level; $74.9961°$ S, $0.094717°$ E) in January 2017. A full description of the methods for the ISOL-ICE ice core can be found in Winton et al. (2019) and only a brief summary is given here. The core was analysed for i) continuous flow analysis (CFA) of nitrate (NO_3^-), sodium (Na) and magnesium (Mg) mass concentrations and electrolytic meltwater conductivity at the British Antarctic Survey (BAS), Cambridge, and ii) discrete sections for the $\delta^{15}N(NO_3^-)$ composition at the Institute of Environmental Geosciences (IGE), University of Grenoble. Here we report the dated section of the ice core from 1227 to 1350 AD (69.8 to 79.4 m) covering the Samalas eruption in 1257. Dating was achieved by annual layer counting of measured concentrations of Na and Mg following previous studies at DML (Göktas et al., 2002; Weller & Wagenbach, 2007; Weller et al., 2008) constrained by well-dated volcanic horizons (further details can be found in Table B1). An age uncertainty of ±3 years is estimated at the base of the ice core. High-resolution sampling for $\delta^{15}N(NO_3^-)$ analysis was carried out i) across volcanic horizons with a sample resolution of 5 to 30 cm, and ii) in 10 cm resolution baseline samples 1 m either side of the volcanic peak. A total of 119 discrete measurements of $\delta^{15}N(NO_3^-)$ are reported here. Discrete $\delta^{15}N(NO_3^-)$ samples were pre-concentrated and analysed using the denitrifier method following Frey et al. (2009)

and Morin et al. (2009). The nitrogen isotopic ratio was referenced against N_2-Air (Mariotti, 1983). We report $^{15}N/^{14}N$ of NO_3^- ($\delta^{15}N(NO_3^-)$) as δ-values: $\delta^{15}N(NO_3^-) = \left(\frac{R_{\text{sample}}}{R_{\text{standard}}} - 1\right)$ where R is the elemental isotopic ratio in the sample and standard respectively. The overall accuracy of the method for $\delta^{15}N(NO_3^-)$ is 3 per mil.

3 Results

3.1 Volcanic perturbations in model

Using the CMIP6 pre-industrial forcings, a year 1850 control run is produced. The control run is 60 years long excluding 10 years of spin up which are discarded. The effect from explosive volcanoes on the stratosphere is investigated by running a series of four volcanic perturbation runs spun off from four different years of the control run to represent the variability arising from different ENSO and QBO states in a similar way to the Pinatubo case study in Section 2.2. The volcanic emissions are prescribed in a similar way to the Pinatubo eruption on 1 September of the first year of the run. Since historical volcanic eruptions are variable and HCl emissions are less well constrained, we develop a matrix of simulations that spans the uncertainty in emissions. The six sets of experiments have one of low SO_2 (10 Tg) or high SO_2 (100 Tg) paired with no HCl, low HCl (0.02 Tg) and high HCl (2 Tg). Changes are plotted as the difference between the average of the four perturbation runs and a climatology derived from the control run.
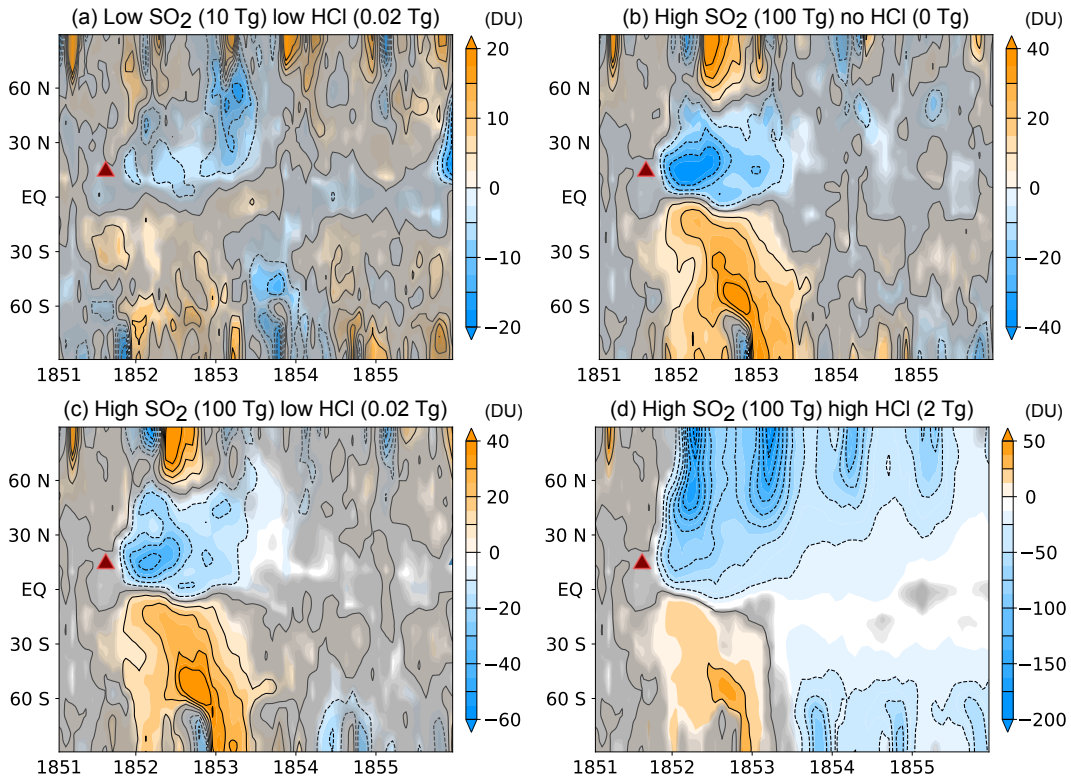
Figure 2. Change in total column ozone (DU) for the pre-industrial volcanic perturbation experiments. The plots show the difference between the average of four ensemble members and a single climatology drawn from a 60 year run. The emission scenarios shown are (a) low SO_2, low HCl case (b) high SO_2, no HCl (c) high SO_2, low HCl and (d) high SO_2, high HCl. The red triangle denotes the location of the injection. Note the different colour scales.

Figure 2 shows the change in total column ozone in the (a) low SO_2 + low HCl, (b) high SO_2 + no HCl, (c) high SO_2 + low HCl and (d) high SO_2 + high HCl cases. The low SO_2 + no HCl case and high SO_2 + no HCl cases are found to be qualitatively similar to two further experiments (not shown): the low SO_2 + low HCl and high SO_2 + low HCl cases, respectively. This is expected since the stratospheric chlorine loading is low (< 0.4 ppbv of HCl over the polar region averaged between 65 to 90° S), similar to a pre-industrial atmosphere and we do not observe large depletion of ozone depletion events by chlorine radicals during spring to form ozone holes.

The low SO_2 + low HCl case in Figure 2(a) represents the ozone response to a Pinatubo-like explosive volcano in a pre-industrial atmosphere. It shows that the changes in TCO are small and dominated by internal variability in most regions. This should be contrasted with the Pinatubo case study shown previously in Figure 1(c) where an eruption of an equivalent magnitude was able to cause significant ozone changes, including an ozone depletion of about 20 DU in the year following the eruption over Antarctica. In contrast, under scenarios of low or no HCl but when the SO_2 emitted is high (Figures 2(b) and (c)), substantial changes in total column ozone are seen for 1.5 years following the eruption. These two cases (high SO_2 and no HCl case, high SO_2 and low HCl) are qualitatively similar suggesting that transport effects still dominate when the amount of HCl is low in a pre-industrial atmosphere and the volcanic chlorine injection is not sufficient to make a significant change to the background stratospheric chlorine loading. The primary impact of a large injection of SO_2 is to locally decrease TCO in the tropics and increase TCO at high latitudes, via the mechanisms described below.

Since chemical, dynamical and radiative processes are coupled in the model, it is difficult to quantify the contribution from individual processes but the results suggest that the main driver of the ozone changes is dynamical in the year following the eruption. The SO_2 aerosol leads to both longwave and shortwave heating in the lower stratosphere (Robock, 2000) resulting in a change in the meridional circulation as shown in Figure 3(a). The increased upwelling brings more ozone-poor tropospheric air into the lower stratosphere leading to lower total column ozone. In contrast, the decreases in upwelling outside the initial SO_2 cloud results in an increase in ozone in the regions polewards of the SO_2 cloud in both hemispheres. Compared to the changes in transport, the changes to the partitioning between radicals and reservoir species for ClO_x, HO_x and NO_x appear to be a second order effect (not shown). The warming in the lower stratosphere results in a warming of the cold point region. This region controls the freeze-drying of water vapour entering the lower stratosphere and warmer temperatures will result in a moistening of the stratosphere and subsequent changes to HO_x chemistry. Changes in SO_2 aerosol also change the partitioning between NO_y and N_2O_5 in the polar regions which can result in ozone changes but these have not been quantified in this study.

In contrast, when a substantial amount of HCl together with SO_2 is injected into the stratosphere (high SO_2 and high HCl case, Figure 2(d)), large, chemical ozone depletion occurs over the polar regions during spring time in the year two to four following the eruption. The initial, low latitude, response still appears to be dynamical but when the injected chlorine reaches polar regions (Figure 3(b)), catalytic destruction of ozone occurs in the polar vortex during spring. The mixing ratio of HCl reaches values of up to 4 ppbv and 1.3 ppbv at 20 km over the North and South poles respectively. These values are comparable to the present day (year 2000) values of the equivalent effective stratospheric chlorine of ~ 3 ppbv. The high SO_2 and high HCl scenario is the one experiment where we observed prolonged ozone destruction occurring over a number of years over Antarctica with a maximum decrease in total column ozone of ~ 90 DU in spring of the second year after the eruption. Over the

North pole, stratospheric ozone is nearly completely removed in the spring for at least four years following the eruption.

The results are sensitive to the date, location and height of the injection in the tropics. A discussion of the sensitivity of eruption source parameters on volcanic radiative forcing can be found in Marshall et al. (2019). In our experiment, the lower branch of the Brewer-Dobson circulation is stronger in the Northern Hemisphere in September and hence the injected chlorine is primarily advected to the North pole in the months following the eruption. It takes about 1.5 years for chlorine to be transported to the South pole. The duration of the response to a volcanic eruption is controlled by stratospheric dynamics and the material that is injected in the lower stratosphere is transported to the troposphere and removed within 2 to 5 years. The injected chlorine will eventually be removed from the polar stratosphere.

In summary, in a pre-industrial atmosphere with low chlorine levels in the stratosphere, we do not detect a significant ozone response to a Pinatubo strength eruption in the model. A large explosive volcano, of similar magnitude to Samalas with no or low HCl produces an increase in total column ozone over Antarctica. The change is short-lived (~ 2 years) and primarily driven by transport changes. In contrast, if a volcanic injection of HCl (2 Tg in our experiments) is able to raise stratospheric chlorine concentrations closer to present day levels, ozone depleting chemical reactions will occur to produce Antarctic ozone depletion in spring as long as sufficient HCl is present. The stratospheric lifetime of chlorine is determined by the age of air and the strength of the stratospheric circulation. When the chlorine reaches the troposphere, it is washed out, giving a lifetime of about 5 years for HCl entering in the shallow branch of the Brewer-Dobson circulation. The increase in surface UV, resulting from ozone depletion, will affect the $\delta^{15}N(NO_3^-)$ ratio in the snow pack. The timing of the change in surface UV could lag, by a number of years, behind that of the volcanic sulphate signal in ice cores, since sulphate arrives via tropospheric and stratospheric transport whilst the UV signal is dependent on stratospheric ozone depletion. An additional difficulty is that the timing of the arrival of the signal depends on the season of the eruption; a quantity that is unknown for most volcanoes over the past 1000 years.
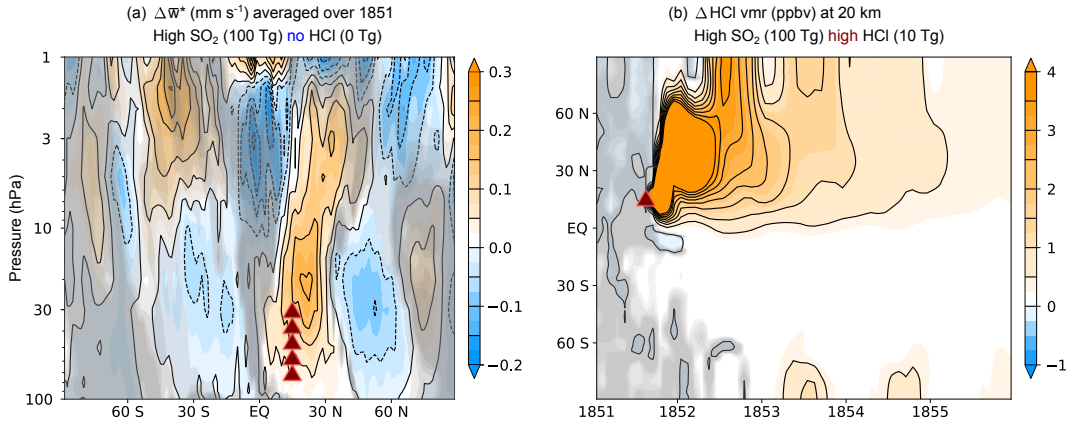
Figure 3. (a) Change in the mean residual vertical velocity for the high SO_2 and no HCl case calculated as the difference between the average over the first year following the eruption of four ensemble members and the mean of the control run to show the dynamical changes. The red triangles represent the location and vertical extent of the volcanic eruption. (b) Change in HCl volume mixing ratio (ppbv) at 20 km for the high SO_2 and high HCl case from the control run to show chemical changes.

3.2 Ice core results
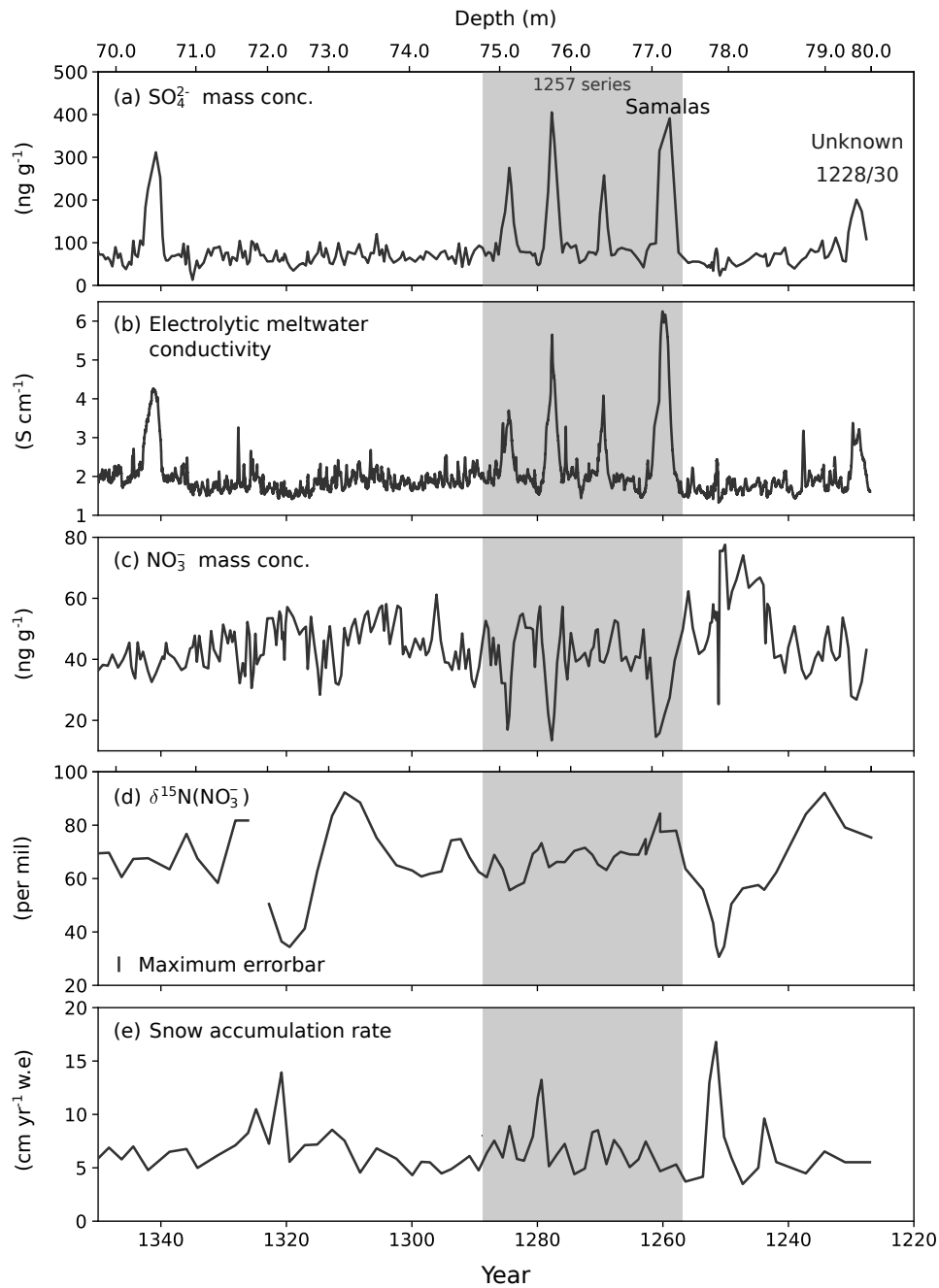
Figure 4. 1227 to 1350 AD section of the ISOL-ICE ice core data from DML, Antarctica. Age is plotted along the bottom and the corresponding ice depth along the top. The vertical grey region marks the dates around the 1257 series of volcanoes. (a) Sulphate mass concentrations. (b) Electrolytic melt water conductivity. (c) Nitrate mass concentration (d) Isotopic ratio of $^{15}N/^{14}N$ of NO_3^- ($\delta^{15}N(NO_3^-)$) given as δ-values. (e) Snow accumulation rate in ($cm\,yr^{-1}$ water equivalent (w.e)). Note that the various quantities are available at different time resolutions depending on the analysis method used.

We expect a tropical volcanic eruption to lead to a sulphate signal in the ice record. The previous modelling studies show that high SO_2 and high HCl eruptions can cause a decrease in TCO which would increase the UV dose reaching the surface at the ice core site. As a result, stronger photolysis would enhance NO_3^- loss, redistribution and recycling from snowpack, decreasing the NO_3^- mass concentration and enriching the $\delta^{15}N(NO_3^-)$ signature.

The ISOL-ICE ice core data from 1227 to 1350 AD is illustrated in Figure 4. The ice core captures a clear signal of the 1257 Samalas series of four volcanic eruptions as indicated by elevated sulphate mass concentrations and electrolytic meltwater conductivity levels above the background in the ice core (Figures 4(a) and (b)). This pattern is consistently observed in ice cores across DML and across the wider Antarctic region (e.g, Hofstede et al. (2004); Göktas et al. (2002)), where sulphate originated from the 1257 series of eruptions, was transported via the stratosphere to Antarctica (Baroni et al., 2008). Nitrate mass concentrations in the ice core decrease coincident with the four large volcanic eruptions (Figure 4(c)). This observation has been reported for other volcanic eruptions in Antarctic and Greenland ice cores, and is thought to occur from the displacement of NO_3^- away from the highly acidic (sulphuric acid) volcanic layers (Wolff, 1995; Laj et al., 1993; Legrand & Kirchner, 1990). This post-depositional process, unrelated to photolysis, leads to the anti-correlation between the sulfate peaks and NO_3^- during the volcanic eruptions. Based on other records of NO_3^- in Antarctica (Pasteris et al., 2014), we expect the NO_3^- mass concentration to be correlated to the accumulation rate outside of the volcanic eruptions. We do not see this positive correlation in the background variability in the ISOL-ICE ice core (Figure 4(c) and (e); $R^2 = 0.04, p < 10^{-3}$ with data from five years either side of the volcanic eruptions is not used). The $\delta^{15}N(NO_3^-)$ is weakly anti-correlated to the accumulation rate (Figure 4(d) and (e); $R^2 = 0.2, p < 10^{-4}$ again with five years either side of the volcanic eruptions removed) as would be expected from spatial transects across Antarctica (Erbland et al., 2015, 2013; Noro et al., 2018; Shi et al., 2018), and sensitivity tests of variable accumulation rate on the $\delta^{15}N(NO_3^-)$ signal at the DML site (Winton et al., 2019).

The accumulation rate is variable at the DML site (2.5 to 11 cm yr^{-1} water equivalent) (Oerter et al., 2000; Sommer et al., 2000) and there is no trend over the last 1000 years. We speculate that changes in the accumulation rate will lead to changes in e-folding depth over time which can account for part of the variability of the $\delta^{15}N(NO_3^-)$ signal (Winton et al., 2019), with a smaller contribution from extreme precipitation events (Turner et al., 2019). The e-folding depth of the local snowpack depends on snow physical properties and contributes to the $\delta^{15}N(NO_3^-)$ signal eventually preserved in local firn and ice (Winton et al., 2019). Unfortunately, the variability of e-folding depth in the past is not known and may be a source of additional noise in the $\delta^{15}N(NO_3^-)$ signal.

We see no enrichment of the $\delta^{15}N(NO_3^-)$ signal above the background variability during the four volcanic eruptions Figure 4(d). We speculate on possible reasons for thus lack of enrichment after the 1257 series. Firstly, the $\delta^{15}N(NO_3^-)$ UV proxy is not sensitive enough to record TCO and concurrent surface UV changes lasting only a few years. Winton et al. (2019) assessed the sensitivity of the $\delta^{15}N(NO_3^-)$ UV proxy to changes in total column ozone using the TRANSITS model (Erbland et al., 2015). We expect that a decrease in the total column ozone of 100 DU, estimated for a large eruption on the magnitude of Samalas (assuming an eruption in September), would result in a 25 per mil increase in $\delta^{15}N(NO_3^-)$ at DML. However, this is below the inter-annual $\delta^{15}N(NO_3^-)$ variability of 30 to 90 per mil at DML (over the period 1227 to 1350 AD), and thus the development of a volcanic induced-large ozone depletion in spring is unlikely to be observed above the natural background $\delta^{15}N(NO_3^-)$ variability. Note that the inter-annual variability of $\delta^{15}N(NO_3^-)$ is larger than the seasonal variability of

about ± 25 per mil of $\delta^{15}N(NO_3^-)$ seen at the bottom of the snow pits in Winton et al. (2019). Despite DML having a relatively low snow accumulation rate, the sensitivity of the $\delta^{15}N(NO_3^-)$ UV proxy is low at this site. Secondly, although we observe a significant decrease in the NO_3^- concentration during the volcanic eruptions, we cannot rule out the possibility that the lower NO_3^- concentrations are due to migration of NO_3^- in acidic layers. Lastly, the impact of acidic volcanic layers on the $\delta^{15}N(NO_3^-)$ has yet to be quantified.

4 Discussion and conclusions

The aim of this paper is to understand the impact on the total column ozone of explosive tropical volcanic eruptions in a low chlorine stratosphere and to search for evidence of these changes in the ice core record over the last 1000 years. We made use of the UM-UKCA chemistry-climate model, with improved heterogeneous reactions and emissions, to model the evolution of ozone after different injections scenarios of SO_2 and HCl representing possible past volcanic eruptions. We then compare the model results to the $\delta^{15}N(NO_3^-)$ isotopic ratio from the recently obtained ISOL-ICE ice core. Winton et al. (2019) and earlier work (Berhanu et al., 2015; Erbland et al., 2015) suggest that it may be possible to use $\delta^{15}N(NO_3^-)$ as a UV proxy for Antarctic ozone changes, after accounting for accumulation rate changes. A decrease in ozone leads to increased surface UV which increases the fractionation of $\delta^{15}N(NO_3^-)$ in the photolytically active region of the snowpack. The resulting $\delta^{15}N(NO_3^-)$ isotopic signal, which integrates the UV signal seen over several years, is then buried. We analyse the $\delta^{15}N(NO_3^-)$ ice core signature around the period of the Samalas eruption to reconstruct past UV changes.

The model experiments show that a "Pinatubo-like" eruption (low SO_2, 10 Tg and low HCl, 0.02 Tg) in a pre-industrial atmosphere does not produce a significant response in ozone over Antarctica (Figure 2(c)) whilst the high SO_2 (100 Tg) volcanoes (with no or low HCl) both produce increases in ozone over Antarctica that are short-lived, lasting about 1.5 years (Figure 2(b) and (c)). The pattern of ozone changes for the latter are primarily caused by transport changes arising from changes to the Brewer-Dobson circulation (Figure 3(a)). In contrast, when the amounts of SO_2 and HCl emitted are both high (high SO_2, 100 Tg and high HCl, 2 Tg) and the HCl loading over the polar regions becomes comparable to present day stratospheric values, our model results show significant ozone depletion over both poles (Figure 2(d)) for at least four years following the eruption. Note that the chemical reactions that destroy ozone are only able to occur when HCl in the stratosphere reaches the polar regions and hence the timing of the springtime ozone depletion depends strongly on the date of the eruption. Since we model the eruption as occurring on 1 September, we find that it takes about 1 year for the injected HCl from the volcano to reach Antarctica (Figure 3(b)). Before the HCl reaches Antarctica, the increase in ozone over the Southern Hemisphere is caused by the same dynamical changes as in the low or no HCl model experiments.

Our results for the ozone response for the high SO_2 and high HCl experiments are quantitatively similar to the experiments by Wade (2018) and Brenna et al. (2019) in terms of the ozone depletion seen over Antarctica. The experiments by Wade (2018) use a coupled atmosphere and ocean with interactive chemistry (HadGEM3-ES model). They explore the range of uncertainty in the emission parameters for the Samalas eruption and vary SO_2 from 94.8 to 142.2 Tg, HCl from 0 to 46.68 Tg and HBr from 0 to 0.263 Tg with a maximum injection height of 34 km. In their highest emission scenario, they observe a decrease of 75% in the global stratospheric ozone and Antarctic ozone depletion (> 240 DU) for six years following the eruption. In the work by Brenna et al. (2019), they impose a Central American explosive volcano in a chemistry climate model (CESM1) in which the effect of sulphuric acid aerosols are

imposed as a modified El Chichòn surface area density forcing equivalent to 30 Tg SO$_2$. The results from their experiment with 2.93 Tg Cl, 9.5 Mt Br at 14°N, 89°W with an injection height of 29.7 hPa on January 1 (their Figure 3(c)) are qualitative similar to our results in Figure 2(d). Brenna et al. (2019) show that the average ozone decreases by more than 120 DU over the polar cap and observe a similar ozone increase over Antarctica in the year after that eruption which is followed by a series of four years with large spring-time ozone depletion.

The results above and the model experiments in this work suggest that if a tropical volcano emits a substantial amount of SO$_2$ and HCl (high SO$_2$, 100 Tg and high HCl, 2 Tg in our case), prolonged ozone depletion, lasting more than four years, will occur over Antarctica. We choose to focus on the ice core record around the Samalas eruption (part of the 1257 series of four volcanoes) since ice core and geochemical evidence suggests that this volcano was the largest in the past 1000 years in terms of SO$_2$ and HCl emissions although there is significant uncertainty in the amount of HCl that was able to reach the stratosphere from this eruption (Halmer et al., 2002). The 1257 series of volcanoes that includes Samalas consists of four eruptions that occur at intervals of 10, 8 and 8 years. If all four eruptions caused ozone depletion, we expect to see a prolonged period of increase in δ^{15}N(NO$_3^-$) in the ice core.

Our record of the isotopic ratio of δ^{15}N(NO$_3^-$) in the ice core around the 1257 series eruptions shows that using δ^{15}N(NO$_3^-$) as a proxy for ozone changes is not able to detect significant prolonged ozone depletion above the level of inter-annual variability. Spatial transects across Antarctica (Noro et al., 2018, and references therein), supported by air snow-photochemistry modelling (TRANSITS) (Winton et al., 2019; Erbland et al., 2015) show a strong non linear dependence of δ^{15}N(NO$_3^-$) on snow accumulation rate. Deeper ice core records in Greenland have observed a dependence of δ^{15}N(NO$_3^-$) and accumulation rate on glacial-interglacial transition timescales (Freyer et al., 1996). In this paper, we present the highest resolution record in ice cores and find that both δ^{15}N(NO$_3^-$) and the accumulation rate show a substantial inter-annual variability (about 30 to 90 per mil and 4 to 18 cm yr^{-1} water equivalent (w.e) respectively in the ice record at $60 - 70$ m depth). However, we do not observe a clear relationship between the two on centennial timescales making it challenging to disentangle the δ^{15}N(NO$_3^-$) signal from other changes such as those in accumulation rate. Winton et al. (2019) show that for a 100 DU change in total column ozone (Figure 2(d)), we expect to see a change of about 25 per mil in δ^{15}N(NO$_3^-$) with a roughly linear relationship. This is below the level of inter-annual variability in δ^{15}N(NO$_3^-$) seen in the ice core of about 60 per mil (the maximum uncertainty in our samples is less than ± 3 per mil over this time period). The snow pack also integrates UV changes over a couple of years and smooths out seasonal variability. For a δ^{15}N(NO$_3^-$) signal to have been detected at the DML site from the 1257 eruptions, we suggest that it would require a prolonged period (several years) of near complete ozone destruction, for instance, during the series of seven stratospheric volcanic eruptions that occurred over a deglaciation ~ 17.7 ka (McConnell et al., 2017). With the additional caveat that the timing and magnitude of ozone changes depends on the season of the eruption and assuming the response scales linearly with forcing, these results suggest that for a signal to be seen above the inter-annual variability, we would need prolonged near complete ozone destruction (over 300 DU). Since we do not see a δ^{15}N(NO$_3^-$) signal of this magnitude in the ice core, this provides a constraint on the magnitude of past ozone changes caused by the 1257 eruptions. We conclude that that it is unlikely that the Samalas 1257 series injected enough HCl to cause complete ozone removal over Antarctica.

In summary, we have evaluated the impact of various explosive tropical volcanic emission scenarios on stratospheric ozone changes in a pre-industrial atmosphere and found that the sign of the ozone change over the polar regions depends on the amount of

Reaction	Uptake coefficient		
	Ice	Nitric acid trihydrate	Sulphate aerosol
$ClONO_2 + HCl \rightarrow Cl_2 + HNO_3$	0.3	0.3	f
$ClONO_2 + H_2O \rightarrow HOCl + HNO_3$	0.3	0.006	f
$HOCl + HCl \rightarrow Cl_2 + H_2O$	0.3	0.3	f
$N_2O_5 + H_2O \rightarrow 2\ HNO_3$	0.03	0.006	0.1
$N_2O_5 + HCl \rightarrow ClNO_2 + HNO_3$	0.03	0.006	0.02
$HOBr + HCl \rightarrow BrCl + H_2O$	0.25	0.25	0.1
$BrONO_2 + HCl \rightarrow BrCl + HNO_3$	0.3	0.3	0.01
$BrONO_2 + H_2O \rightarrow HOBr + HNO_3$	0.3	0.001	0.01
$HOBr + HBr \rightarrow Br_2 + H_2O$	0.25	0.25	0.1
$HOCl + HBr \rightarrow BrCl + H_2O$	0.25	0.25	0.02
$ClONO_2 + HBr \rightarrow BrCl + HNO_3$	0.56	0.56	0.02
$BrONO_2 + HBr \rightarrow Br_2 + HNO_3$	0.3	0.3	0.01
$N_2O_5 + HBr \rightarrow BrNO_2 + HNO_3$	0.05	0.001	0.02

f denotes uptake coefficients calculated using the method in Shi et al. (2001).
Table A1. New heterogeneous reactions added to the UKCA module together with the uptake coefficients.

HCl injected by the eruption. $\delta^{15}N(NO_3^-)$ can theoretically be used as a proxy for UV and thus has the potential to indicate changes in past TCO. Changes in $\delta^{15}N(NO_3^-)$ could be positive or negative (indicating either increases or decreased in TCO) depending on the type of volcanic eruption and they are unlikely to be synchronous with sulphate peaks because of different transport pathways and the different timings of the ozone changes. Using a novel high resolution $\delta^{15}N(NO_3^-)$ ice core record, we are unable to detect a signal from the largest volcanic eruption (1257 series) in the past 1000 years as there is a large inter-annual variability in the $\delta^{15}N(NO_3^-)$ record. We recommend that future studies of this nature should first understand why the $\delta^{15}N(NO_3^-)$ record has a large variability at DML site if $\delta^{15}N(NO_3^-)$ is to be used to constrain the ozone change. A site with lower variability than 25 per mil in $\delta^{15}N(NO_3^-)$ could be considered although increasing the sensitivity of the UV proxy by choosing a site with lower annual accumulation comes at the expense of reduced time resolution making it less likely to resolve volcanic eruptions.

Appendix A Model improvements

A1 Heterogeneous and photolysis reactions

Table A1 lists the new heterogeneous reactions added to the UKCA module together with the uptake coefficients on ice, nitric acid trihydrate and sulfate aerosol. This can be compared to Table 1 in Dennison et al. (2019). We use the method in Shi et al. (2001) to calculate the values of the uptake coefficients that are not constant and are denoted by f in Table A1.

A2 Bromocarbon emissions

The emission flux datasets of the five very short lived bromocarbon species (CH_3Br, CH_2BrCl, CH_2Br_2, $CHBr_2Cl$, $CHBrCl_2$) are explicitly included as emission files. These are similar to the ones used in Yang et al. (2014), which are based on

Volcano	Eruption date	Arrival date	Peak Depth (m)	Start Depth (m)
Kuwae[a]	1450	1454	61.01	61.13
1285[b]	1285	1285	75.12	75.22
1277[b]	1277	1277	75.77	75.9
1269[b]	1269	1269	76.41	77.46
Samalas 1257[b]	1257	1259	77.12	77.23
Unknown 1228/30[b]	1229	1229	79.33	79.43

[a] Zielinski et al. (1994) [b] Langway Jr. et al. (1995)

Table B1. Volcanic horizons identified from the sulfate and electrical meltwater conductivity records. Eruption date of the volcano and arrival dates of the sulfate in the ice core are obtained from Zielinski et al. (1994) and Langway Jr. et al. (1995) except for the Unknown 1228/30 volcano where the precise eruption date is not known. We choose 1229 as the eruption and arrival date for dating purposes.

the original work (scenario 5) of Warwick et al. (2006), except for the emissions of CH_2Br_2. The emissions of CH_2Br_2 were scaled to give a total emission of $57\,\mathrm{Gg\,yr^{-1}}$, corresponding to 50% of the original flux and in better agreement with Liang et al. (2010) and Ordóñez et al. (2012). The combined effect of the bromocarbons is to provide $\sim$ 5pptv of inorganic bromine to the stratosphere (Yang et al., 2014) in a pre-industrial atmosphere.

Appendix B Ice core analysis

Table B1 shows the volcanic horizons identified from the sulfate and electrical meltwater conductivity records in the ISOL-ICE ice core.

References

Aquila, V., Oman, L. D., Stolarski, R. S., Colarco, P. R., & Newman, P. A.   (2012). Dispersion of the volcanic sulfate cloud from a mount pinatubolike erup- tion.   *Journal of Geophysical Research: Atmospheres*, *117*(D6).   Retrieved from `https://agupubs.onlinelibrary.wiley.com/doi/abs/10.1029/2011JD016968` doi: 10.1029/2011JD016968

Baroni, M., Savarino, J., Cole-Dai, J., Rai, V. K., & Thiemens, M. H.   (2008). Anomalous sulfur isotope compositions of volcanic sulfate over the last millen- nium in antarctic ice cores.   *Journal of Geophysical Research: Atmospheres*, *113*(D20).   Retrieved from `https://agupubs.onlinelibrary.wiley.com/doi/abs/10.1029/2008JD010185` doi: 10.1029/2008JD010185

Berhanu, T. A., Meusinger, C., Erbland, J., Jost, R., Bhattacharya, S. K., John- son, M. S., & Savarino, J.   (2014).   Laboratory study of nitrate photolysis in antarctic snow. ii. isotopic effects and wavelength dependence.   *The Journal of Chemical Physics*, *140*(24), 244306.   Retrieved from `https://doi.org/10.1063/1.4882899` doi: 10.1063/1.4882899

Berhanu, T. A., Savarino, J., Erbland, J., Vicars, W. C., Preunkert, S., Martins, J. F., & Johnson, M. S.   (2015).   Isotopic effects of nitrate photochemistry in snow: a field study at dome c, antarctica. *Atmospheric Chemistry and Physics*, *15*(19), 11243–11256.   Retrieved from `https://www.atmos-chem-phys.net/15/11243/2015/` doi: 10.5194/acp-15-11243-2015

Bian, H., & Prather, M. J. (2002, 01). Fast-j2: Accurate simulation of stratospheric photolysis in global chemical models.   *Journal of Atmospheric Chemistry*, *41*(3), 281–296. Retrieved from `https://doi.org/10.1023/A:1014980619462` doi: 10.1023/A:1014980619462

Brenna, H., Kutterolf, S., & Krger, K.   (2019).   Global ozone depletion and increase of UV radiation caused by pre-industrial tropical volcanic eruptions.   *Scientific Reports*, *9*(1), 9435. doi: 10.1038/s41598-019-45630-0

Butchart, N., Charlton-Perez, A. J., Cionni, I., Hardiman, S. C., Haynes, P. H., Krger, K., . . . Yamashita, Y. (2011). Multimodel climate and variability of the stratosphere.   *Journal of Geophysical Research: Atmospheres*, *116*(D5).   doi: 10.1029/2010JD014995

Chapman, S. (1930). A theory of upper-atmospheric ozone. *Memories of Royal Me- teorological Society*, *III*(26), 103-125.

Crutzen, P. J.   (1970).   The influence of nitrogen oxides on the atmospheric ozone content.   *Quarterly Journal of the Royal Meteorological Society*, *96*(408), 320- 325. doi: 10.1002/qj.49709640815

Dennison, F., Keeble, J., Morgenstern, O., Zeng, G., Abraham, N. L., & Yang, X. (2019).   Improvements to stratospheric chemistry scheme in the um-ukca (v10.7) model: solar cycle and heterogeneous reactions.   *Geoscientific Model Development*, *12*(3), 1227–1239.   Retrieved from `https://www.geosci-model -dev.net/12/1227/2019/` doi: 10.5194/gmd-12-1227-2019

Erbland, J., Savarino, J., Morin, S., France, J. L., Frey, M. M., & King, M. D. (2015).   Air-snow transfer of nitrate on the east antarctic plateau; part 2: An isotopic model for the interpretation of deep ice-core records.   *At- mospheric Chemistry and Physics*, *15*(20), 12079–12113.   Retrieved from

https://www.atmos-chem-phys.net/15/12079/2015/ doi: 10.5194/acp-15-12079-2015

Erbland, J., Vicars, W. C., Savarino, J., Morin, S., Frey, M. M., Frosini, D., ... Martins, J. M. F. (2013). Air-snow transfer of nitrate on the east antarctic plateau; part 1: Isotopic evidence for a photolytically driven dynamic equilibrium in summer. *Atmospheric Chemistry and Physics*, *13*(13), 6403–6419. Retrieved from https://www.atmos-chem-phys.net/13/6403/2013/ doi: 10.5194/acp-13-6403-2013

Eyring, V., Bony, S., Meehl, G. A., Senior, C. A., Stevens, B., Stouffer, R. J., & Taylor, K. E. (2016). Overview of the coupled model intercomparison project phase 6 (cmip6) experimental design and organization. *Geoscientific Model Development*, *9*(5), 1937–1958. Retrieved from https://www.geosci-model-dev.net/9/1937/2016/ doi: 10.5194/gmd-9-1937-2016

Eyring, V., Cionni, I., Bodeker, G. E., Charlton-Perez, A. J., Kinnison, D. E., Scinocca, J. F., ... Yamashita, Y. (2010). Multi-model assessment of stratospheric ozone return dates and ozone recovery in ccmval-2 models. *Atmospheric Chemistry and Physics*, *10*(19), 9451–9472. doi: 10.5194/acp-10-9451-2010

Frey, M. M., Savarino, J., Morin, S., Erbland, J., & Martins, J. M. F. (2009). Photolysis imprint in the nitrate stable isotope signal in snow and atmosphere of east antarctica and implications for reactive nitrogen cycling. *Atmospheric Chemistry and Physics*, *9*(22), 8681–8696. Retrieved from https://www.atmos-chem-phys.net/9/8681/2009/ doi: 10.5194/acp-9-8681-2009

Freyer, H. D., Kobel, K., Delmas, R. J., Kley, D., & Legrand, M. R. (1996). First results of 15n/14n ratios in nitrate from alpine and polar ice cores. *Tellus B: Chemical and Physical Meteorology*, *48*(1), 93-105. Retrieved from https://doi.org/10.3402/tellusb.v48i1.15671 doi: 10.3402/tellusb.v48i1.15671

Göktas, F., Fischer, H., Oerter, H., Weller, R., Sommer, S., & Miller, H. (2002). A glacio-chemical characterization of the new epica deep-drilling site on amundsenisen, dronning maud land, antarctica. *Annals of Glaciology*, *35*, 347–354. doi: 10.3189/172756402781816474

Halmer, M., Schmincke, H.-U., & Graf, H.-F. (2002). The annual volcanic gas input into the atmosphere, in particular into the stratosphere: a global data set for the past 100 years. *Journal of Volcanology and Geothermal Research*, *115*(3), 511 - 528. doi: https://doi.org/10.1016/S0377-0273(01)00318-3

Harris, N. R. P., Hassler, B., Tummon, F., Bodeker, G. E., Hubert, D., Petropavlovskikh, I., ... Zawodny, J. M. (2015). Past changes in the vertical distribution of ozone part 3: Analysis and interpretation of trends. *Atmospheric Chemistry and Physics*, *15*(17), 9965–9982. Retrieved from https://www.atmos-chem-phys.net/15/9965/2015/ doi: 10.5194/acp-15-9965-2015

Hofstede, C. M., Roderik, S. v. d. W., Kaspers, K. A., van den Broeke, M. R., Karlöf, L., Winther, J.-G., ... Wilhelms, F. (2004). Firn accumulation records for the past 1000 years on the basis of dielectric profiling of six cores from dronning maud land, antarctica. *Journal of Glaciology*, *50*(169), 279–291. doi: 10.3189/172756504781830169

Johnston, H. (1971). Reduction of stratospheric ozone by nitrogen oxide catalysts from supersonic transport exhaust. *Science*, *173*(3996), 517–522. doi: 10.1126/science.173.3996.517

Kutterolf, S., Hansteen, T., Appel, K., Freundt, A., Krger, K., Prez, W., & Wehrmann, H. (2013). Combined bromine and chlorine release from large explosive volcanic eruptions: A threat to stratospheric ozone? *Geology*, *41*(6), 707-710. Retrieved from https://doi.org/10.1130/G34044.1 doi: 10.1130/G34044.1

Laj, P., Palais, J. M., Gardner, J. E., & Sigurdsson, H. (1993). Modified hno3 seasonality in volcanic layers of a polar ice core: Snow-pack effect or pho-

tochemical perturbation? *Journal of Atmospheric Chemistry*, *16*(3), 219–230. Retrieved from https://doi.org/10.1007/BF00696897 doi: 10.1007/BF00696897

Langematz, U., Tully (Lead authors), M., Calvo, N., Dameris, M., de Laat, A., Klekociuk, A., . . . Young, P. (2018). Update on ozone-depleting substances (odss) and other gases of interest to the montreal protocol. In *Scientific assessment of ozone depletion* (chap. 4). World Meteorological Organization, Geneva, Switzerland.

Langway Jr., C. C., Osada, K., Clausen, H. B., Hammer, C. U., & Shoji, H. (1995). A 10-century comparison of prominent bipolar volcanic events in ice cores. *Journal of Geophysical Research: Atmospheres*, *100*(D8), 16241–16247. Retrieved from https://agupubs.onlinelibrary.wiley.com/doi/abs/10.1029/95JD01175 doi: 10.1029/95JD01175

Lary, D. J., & Pyle, J. A. (1991). Diffuse radiation, twilight, and photochemistry. I, II. *Journal of Atmospheric Chemistry*, *13*, 373–406. doi: 10.1007/BF00057753

Legrand, M. R., & Kirchner, S. (1990). Origins and variations of nitrate in south polar precipitation. *Journal of Geophysical Research: Atmospheres*, *95*(D4), 3493-3507. Retrieved from https://agupubs.onlinelibrary.wiley.com/doi/abs/10.1029/JD095iD04p03493 doi: 10.1029/JD095iD04p03493

Lehner, F., Schurer, A. P., Hegerl, G. C., Deser, C., & Frölicher, T. L. (2016). The importance of enso phase during volcanic eruptions for detection and attribution. *Geophysical Research Letters*, *43*(6), 2851–2858. Retrieved from https://agupubs.onlinelibrary.wiley.com/doi/abs/10.1002/2016GL067935 doi: 10.1002/2016GL067935

Liang, Q., Stolarski, R. S., Kawa, S. R., Nielsen, J. E., Douglass, A. R., Rodriguez, J. M., . . . Ott, L. E. (2010). Finding the missing stratospheric br_y: a global modeling study of $chbr_3$ and ch_2br_2. *Atmospheric Chemistry and Physics*, *10*(5), 2269–2286. Retrieved from https://www.atmos-chem-phys.net/10/2269/2010/ doi: 10.5194/acp-10-2269-2010

Mann, G. W., Carslaw, K. S., Spracklen, D. V., Ridley, D. A., Manktelow, P. T., Chipperfield, M. P., . . . Johnson, C. E. (2010). Description and evaluation of glomap-mode: a modal global aerosol microphysics model for the ukca composition-climate model. *Geoscientific Model Development*, *3*(2), 519–551. Retrieved from https://www.geosci-model-dev.net/3/519/2010/ doi: 10.5194/gmd-3-519-2010

Mariotti, A. (1983). Atmospheric nitrogen is a reliable standard for natural 15N abundance measurements. *Nature*, *303*(5919), 685–687. doi: https://doi.org/10.1038/303685a0

Marshall, L., Johnson, J. S., Mann, G. W., Lee, L., Dhomse, S. S., Regayre, L., . . . Schmidt, A. (2019). Exploring how eruption source parameters affect volcanic radiative forcing using statistical emulation. *Journal of Geophysical Research: Atmospheres*, *124*(2), 964–985. Retrieved from https://agupubs.onlinelibrary.wiley.com/doi/abs/10.1029/2018JD028675 doi: 10.1029/2018JD028675

McConnell, J. R., Burke, A., Dunbar, N. W., Köhler, P., Thomas, J. L., Arienzo, M. M., . . . Winckler, G. (2017). Synchronous volcanic eruptions and abrupt climate change ~17.7 ka plausibly linked by stratospheric ozone depletion. *Proceedings of the National Academy of Sciences*, *114*(38), 10035–10040. doi: 10.1073/pnas.1705595114

McLandress, C., Shepherd, T. G., Polavarapu, S., & Beagley, S. R. (2012). Is missing orographic gravity wave drag near 60s the cause of the stratospheric zonal wind biases in chemistryclimate models? *Journal of the Atmospheric Sciences*, *69*(3), 802-818. doi: 10.1175/JAS-D-11-0159.1

Mills, M. J., Schmidt, A., Easter, R., Solomon, S., Kinnison, D. E., Ghan, S. J.,

785   ... Gettelman, A. (2016). Global volcanic aerosol properties derived
786   from emissions, 19902014, using cesm1(waccm). *Journal of Geophysi-*
787   *cal Research: Atmospheres*, *121*(5), 2332–2348. Retrieved from `https://`
788   `agupubs.onlinelibrary.wiley.com/doi/abs/10.1002/2015JD024290` doi:
789   10.1002/2015JD024290

790 Ming, A. (2020). *Isol-ice: Volcanic eruptions in the ukca vn10.9 model*
791   *with additional reactions.* `https://catalogue.ceda.ac.uk/uuid/`
792   `c78f77ba752d44598baabb7169651239.` Centre for Environmental Data Analy-
793   sis. 6 May 2020.

794 Morgenstern, O., Braesicke, P., O'Connor, F. M., Bushell, A. C., Johnson, C. E.,
795   Osprey, S. M., & Pyle, J. A. (2009). Evaluation of the new ukca climate-
796   composition model; part 1: The stratosphere. *Geoscientific Model Develop-*
797   *ment*, *2*(1), 43–57. Retrieved from `https://www.geosci-model-dev.net/2/`
798   `43/2009/` doi: 10.5194/gmd-2-43-2009

799 Morin, S., Savarino, J., Frey, M. M., Domine, F., Jacobi, H.-W., Kaleschke, L., &
800   Martins, J. M. F. (2009). Comprehensive isotopic composition of atmospheric
801   nitrate in the atlantic ocean boundary layer from 65°s to 79°n. *Journal of*
802   *Geophysical Research: Atmospheres*, *114*(D5). Retrieved from `https://`
803   `agupubs.onlinelibrary.wiley.com/doi/abs/10.1029/2008JD010696` doi:
804   10.1029/2008JD010696

805 Neu, J. L., Prather, M. J., & Penner, J. E. (2007). Global atmospheric chemistry:
806   Integrating over fractional cloud cover. *Journal of Geophysical Research: At-*
807   *mospheres*, *112*(D11). Retrieved from `https://agupubs.onlinelibrary`
808   `.wiley.com/doi/abs/10.1029/2006JD008007` doi: 10.1029/2006JD008007

809 Noro, K., Hattori, S., Uemura, R., Fukui, K., Hirabayashi, M., Kawamura, K.,
810   ... Yoshida, N. (2018). Spatial variation of isotopic compositions of snow-
811   pack nitrate related to post-depositional processes in eastern dronning maud
812   land, east antarctica. *GEOCHEMICAL JOURNAL*, *52*(2), e7–e14. doi:
813   10.2343/geochemj.2.0519

814 O'Connor, F. M., Johnson, C. E., Morgenstern, O., Abraham, N. L., Braesicke,
815   P., Dalvi, M., ... Pyle, J. A. (2014). Evaluation of the new ukca climate-
816   composition model – part 2: The troposphere. *Geoscientific Model Develop-*
817   *ment*, *7*(1), 41–91. doi: 10.5194/gmd-7-41-2014

818 Oerter, H., Wilhelms, F., Jung-Rothenhäusler, F., Göktas, F., Miller, H., Graf, W.,
819   & Sommer, S. (2000). Accumulation rates in dronning maud land, antarctica,
820   as revealed by dielectric-profiling measurements of shallow firn cores. *Annals of*
821   *Glaciology*, *30*, 2734. doi: 10.3189/172756400781820705

822 Ordóñez, C., Lamarque, J.-F., Tilmes, S., Kinnison, D. E., Atlas, E. L., Blake,
823   D. R., ... Saiz-Lopez, A. (2012). Bromine and iodine chemistry in a global
824   chemistry-climate model: description and evaluation of very short-lived
825   oceanic sources. *Atmospheric Chemistry and Physics*, *12*(3), 1423–1447.
826   Retrieved from `https://www.atmos-chem-phys.net/12/1423/2012/` doi:
827   10.5194/acp-12-1423-2012

828 Osprey, S. M., Gray, L. J., Hardiman, S. C., Butchart, N., & Hinton, T. J. (2013).
829   Stratospheric variability in twentieth-century cmip5 simulations of the met
830   office climate model: High top versus low top. *Journal of Climate*, *26*(5),
831   1595–1606. Retrieved from `https://doi.org/10.1175/JCLI-D-12-00147.1`
832   doi: 10.1175/JCLI-D-12-00147.1

833 Pasteris, D., McConnell, J. R., Edwards, R., Isaksson, E., & Albert, M. R. (2014).
834   Acidity decline in antarctic ice cores during the little ice age linked to changes
835   in atmospheric nitrate and sea salt concentrations. *Journal of Geophysi-*
836   *cal Research: Atmospheres*, *119*(9), 5640-5652. Retrieved from `https://`
837   `agupubs.onlinelibrary.wiley.com/doi/abs/10.1002/2013JD020377` doi:
838   10.1002/2013JD020377

839 Poberaj, C. S., Staehelin, J., & Brunner, D. (2011). Missing stratospheric ozone

decrease at southern hemisphere middle latitudes after mt. pinatubo: A dynamical perspective. *Journal of the Atmospheric Sciences*, *68*(9), 1922–1945. Retrieved from `https://doi.org/10.1175/JAS-D-10-05004.1` doi: 10.1175/JAS-D-10-05004.1

Robock, A. (2000). Volcanic eruptions and climate. *Reviews of Geophysics*, *38*(2), 191–219. Retrieved from `https://agupubs.onlinelibrary.wiley.com/doi/abs/10.1029/1998RG000054` doi: 10.1029/1998RG000054

Robock, A., & Oppenheimer, C. (Eds.). (2003). *Volcanism and the Earth's Atmosphere* (Vol. 139). Washington DC American Geophysical Union Geophysical Monograph Series. doi: 10.1029/GM139

Severi, M., Becagli, S., Castellano, E., Morganti, A., Traversi, R., Udisti, R., . . . Steffensen, J. P. (2007). Synchronisation of the edml and edc ice cores for the last 52 kyr by volcanic signature matching. *Climate of the Past*, *3*(3), 367–374. Retrieved from `https://www.clim-past.net/3/367/2007/` doi: 10.5194/cp-3-367-2007

Shi, G., Buffen, A., Ma, H., Hu, Z., Sun, B., Li, C., . . . Hastings, M. (2018). Distinguishing summertime atmospheric production of nitrate across the east antarctic ice sheet. *Geochimica et Cosmochimica Acta*, *231*, 1 - 14. Retrieved from `http://www.sciencedirect.com/science/article/pii/S0016703718301856` doi: https://doi.org/10.1016/j.gca.2018.03.025

Shi, G., Chai, J., Zhu, Z., Hu, Z., Chen, Z., Yu, J., . . . Hastings, M. (2019). Isotope fractionation of nitrate during volatilization in snow: A field investigation in antarctica. *Geophysical Research Letters*, *46*(6), 3287–3297. Retrieved from `https://agupubs.onlinelibrary.wiley.com/doi/abs/10.1029/2019GL081968` doi: 10.1029/2019GL081968

Shi, Q., Jayne, J. T., Kolb, C. E., Worsnop, D. R., & Davidovits, P. (2001). Kinetic model for reaction of clono2 with h2o and hcl and hocl with hcl in sulfuric acid solutions. *Journal of Geophysical Research: Atmospheres*, *106*(D20), 24259-24274. Retrieved from `https://agupubs.onlinelibrary.wiley.com/doi/abs/10.1029/2000JD000181` doi: 10.1029/2000JD000181

Solomon, S. (1999). Stratospheric ozone depletion: A review of concepts and history. *Reviews of Geophysics*, *37*(3), 275-316. Retrieved from `https://agupubs.onlinelibrary.wiley.com/doi/abs/10.1029/1999RG900008` doi: 10.1029/1999RG900008

Sommer, S., Appenzeller, C., Röthlisberger, R., Hutterli, M. A., Stauffer, B., Wagenbach, D., . . . Mulvaney, R. (2000). Glacio-chemical study spanning the past 2 kyr on three ice cores from dronning maud land, antarctica: 1. annually resolved accumulation rates. *Journal of Geophysical Research: Atmospheres*, *105*(D24), 29411-29421. Retrieved from `https://agupubs.onlinelibrary.wiley.com/doi/abs/10.1029/2000JD900449` doi: 10.1029/2000JD900449

Sommer, S., Wagenbach, D., Mulvaney, R., & Fischer, H. (2000). Glacio-chemical study spanning the past 2 kyr on three ice cores from dronning maud land, antarctica: 2. seasonally resolved chemical records. *Journal of Geophysical Research: Atmospheres*, *105*(D24), 29423-29433. Retrieved from `https://agupubs.onlinelibrary.wiley.com/doi/abs/10.1029/2000JD900450` doi: 10.1029/2000JD900450

Stevenson, S., Fasullo, J. T., Otto-Bliesner, B. L., Tomas, R. A., & Gao, C. (2017). Role of eruption season in reconciling model and proxy responses to tropical volcanism. *Proceedings of the National Academy of Sciences*, *114*(8), 1822–1826. Retrieved from `https://www.pnas.org/content/114/8/1822` doi: 10.1073/pnas.1612505114

Telford, P., Braesicke, P., Morgenstern, O., & Pyle, J. (2009). Reassessment of causes of ozone column variability following the eruption of mount pinatubo using a nudged ccm. *Atmospheric Chemistry and Physics*, *9*(13), 4251–4260.

Retrieved from https://www.atmos-chem-phys.net/9/4251/2009/ doi: 10.5194/acp-9-4251-2009

Telford, P. J., Abraham, N. L., Archibald, A. T., Braesicke, P., Dalvi, M., Morgenstern, O., . . . Pyle, J. A. (2013). Implementation of the fast-jx photolysis scheme (v6.4) into the ukca component of the metum chemistry-climate model (v7.3). *Geoscientific Model Development*, *6*(1), 161–177. Retrieved from https://www.geosci-model-dev.net/6/161/2013/ doi: 10.5194/gmd-6-161-2013

Textor, C., Graf, H.-F., Herzog, M., & Oberhuber, J. M. (2003). Injection of gases into the stratosphere by explosive volcanic eruptions. *Journal of Geophysical Research: Atmospheres*, *108*(D19). Retrieved from https://agupubs.onlinelibrary.wiley.com/doi/abs/10.1029/2002JD002987 doi: 10.1029/2002JD002987

Theys, N., De Smedt, I., Van Roozendael, M., Froidevaux, L., Clarisse, L., & Hendrick, F. (2014). First satellite detection of volcanic oclo after the eruption of puyehue-cordòn caulle. *Geophysical Research Letters*, *41*(2), 667–672. Retrieved from https://agupubs.onlinelibrary.wiley.com/doi/abs/10.1002/2013GL058416 doi: 10.1002/2013GL058416

Tie, X., & Brasseur, G. (1995). The response of stratospheric ozone to volcanic eruptions: Sensitivity to atmospheric chlorine loading. *Geophysical Research Letters*, *22*, 3035-3038. doi: 10.1029/95GL03057

Timmreck, C. (2012). Modeling the climatic effects of large explosive volcanic eruptions. *WIREs Climate Change*, *3*(6), 545-564. doi: 10.1002/wcc.192

Timmreck, C., Mann, G. W., Aquila, V., Hommel, R., Lee, L. A., Schmidt, A., . . . Weisenstein, D. (2018). The interactive stratospheric aerosol model intercomparison project (isa-mip): motivation and experimental design. *Geoscientific Model Development*, *11*(7), 2581–2608. Retrieved from https://www.geosci-model-dev.net/11/2581/2018/ doi: 10.5194/gmd-11-2581-2018

Toohey, M., & Sigl, M. (2017). Volcanic stratospheric sulfur injections and aerosol optical depth from 500 bce to 1900 ce. *Earth System Science Data*, *9*(2), 809–831. Retrieved from https://www.earth-syst-sci-data.net/9/809/2017/ doi: 10.5194/essd-9-809-2017

Turner, J., Phillips, T., Thamban, M., Rahaman, W., Marshall, G. J., Wille, J. D., . . . Lachlan-Cope, T. (2019). The dominant role of extreme precipitation events in antarctic snowfall variability. *Geophysical Research Letters*, *46*(6), 3502-3511. Retrieved from https://agupubs.onlinelibrary.wiley.com/doi/abs/10.1029/2018GL081517 doi: 10.1029/2018GL081517

Vidal, C. M., Métrich, N., Komorowski, J.-C., Pratomo, I., Michel, A., Kartadinata, N., . . . Lavigne, F. (2016). The 1257 samalas eruption (lombok, indonesia): the single greatest stratospheric gas release of the common era. *Scientific reports*, *6*, 34868. doi: 10.1038/srep34868

Wade, D. C. (2018). *Investigating palaeoatmospheric composition-climate interactions* (Doctoral dissertation, University of Cambridge). doi: 10.17863/CAM .30363

Wallace, L., & Livingston, W. (1992). The effect of the pinatubo cloud on hydrogen chloride and hydrogen fluoride. *Geophysical Research Letters*, *19*(12), 1209–1209. Retrieved from https://agupubs.onlinelibrary.wiley.com/doi/abs/10.1029/92GL01112 doi: 10.1029/92GL01112

Walters, D., Baran, A. J., Boutle, I., Brooks, M., Earnshaw, P., Edwards, J., . . . Zerroukat, M. (2019). The met office unified model global atmosphere 7.0/7.1 and jules global land 7.0 configurations. *Geoscientific Model Development*, *12*(5), 1909–1963. doi: 10.5194/gmd-12-1909-2019

Warwick, N. J., Pyle, J. A., Carver, G. D., Yang, X., Savage, N. H., O'Connor, F. M., & Cox, R. A. (2006). Global modeling of biogenic bromocar-

bons. *Journal of Geophysical Research: Atmospheres*, *111*(D24). Retrieved from https://agupubs.onlinelibrary.wiley.com/doi/abs/10.1029/ 2006JD007264 doi: 10.1029/2006JD007264

Weller, R., & Wagenbach, D. (2007). Year-round chemical aerosol records in continental antarctica obtained by automatic samplings. *Tellus B: Chemical and Physical Meteorology*, *59*(4), 755-765. Retrieved from https://doi.org/ 10.1111/j.1600-0889.2007.00293.x doi: 10.1111/j.1600-0889.2007.00293.x

Weller, R., Wöltjen, J., Piel, C., Resenberg, R., Wagenbach, D., König-Langlo, G., & Kriews, M. (2008). Seasonal variability of crustal and marine trace elements in the aerosol at neumayer station, antarctica. *Tellus B: Chemical and Physical Meteorology*, *60*(5), 742-752. Retrieved from https://doi.org/10.1111/ j.1600-0889.2008.00372.x doi: 10.1111/j.1600-0889.2008.00372.x

Wild, O., Zhu, X., & Prather, M. J. (2000, 01). Fast-j: Accurate simulation of in- and below-cloud photolysis in tropospheric chemical models. *Journal of Atmospheric Chemistry*, *37*(3), 245–282. Retrieved from https://doi.org/ 10.1023/A:1006415919030 doi: 10.1023/A:1006415919030

Winton, V. H. L., Ming, A., Caillon, N., Hauge, L., Jones, A. E., Savarino, J., . . . Frey, M. M. (2019). Deposition, recycling and archival of nitrate stable isotopes between the air-snow interface: comparison between dronning maud land and dome c, antarctica. *Atmospheric Chemistry and Physics Discussions*, *2019*, 1–44. Retrieved from https://www.atmos-chem-phys-discuss.net/ acp-2019-669/ doi: 10.5194/acp-2019-669

Winton, V. H. L. W., Caillon, N., Hauge, L., Mulvaney, R., Rix, J., Savarino, J., . . . Frey, M. (2019). *Ice core chemistry, conductivity, and stable nitrate isotopic composition of the samalas eruption in 1259 from the isol-ice ice core, dronning maud land, antarctica, version 1.0.* https://doi.org/10.5285/ d9a74ea7-2a1a-4068-847e-5bc9f51947c5. UK Polar Data Centre, Natural Environment Research Council, UK Research and Innovation. doi: 10.5285/d9a74ea7-2a1a-4068-847e-5bc9f51947c5

Wolff, E. W. (1995). Nitrate in polar ice. In R. J. Delmas (Ed.), *Ice core studies of global biogeochemical cycles* (pp. 195–224). Berlin: Springer-Verlag. Retrieved from http://nora.nerc.ac.uk/id/eprint/515900/

Yang, X., Abraham, N. L., Archibald, A. T., Braesicke, P., Keeble, J., Telford, P. J., . . . Pyle, J. A. (2014). How sensitive is the recovery of stratospheric ozone to changes in concentrations of very short-lived bromocarbons? *Atmospheric Chemistry and Physics*, *14*(19), 10431–10438. Retrieved from https://www.atmos-chem-phys.net/14/10431/2014/ doi: 10.5194/acp-14-10431-2014

Zanchettin, D., Khodri, M., Timmreck, C., Toohey, M., Schmidt, A., Gerber, E. P., . . . Tummon, F. (2016). The model intercomparison project on the climatic response to volcanic forcing (volmip): experimental design and forcing input data for cmip6. *Geoscientific Model Development*, *9*(8), 2701–2719. Retrieved from https://www.geosci-model-dev.net/9/2701/2016/ doi: 10.5194/gmd-9-2701-2016

Zielinski, G. A., Mayewski, P. A., Meeker, L. D., Whitlow, S., Twickler, M. S., Morrison, M., . . . Alley, R. B. (1994). Record of volcanism since 7000 b.c. from the gisp2 greenland ice core and implications for the volcano-climate system. *Science*, *264*(5161), 948–952. Retrieved from https://science.sciencemag .org/content/264/5161/948 doi: 10.1126/science.264.5161.948